

# Understanding the factors affecting the self-heating process of compost piles: Two-dimensional analysis

T. Luangwilai<sup>1</sup>

H. S. Sidhu<sup>2</sup>

M. I. Nelson<sup>3</sup>

(Received 30 January 2022; revised 21 April 2022)

## Abstract

Industrial compost piles contain large volumes of bulk organic materials. Normally, there are two main heat generation processes—oxidation of cellulosic materials and biological activity within the compost pile. Biological heating occurs at a lower temperature range, but it may ‘kick-start’ the oxidation reaction. Nevertheless, biological heating is desirable and is a key component in composting operations. However, there are cases when the temperature within the compost piles increases beyond the ignition temperature of cellulosic materials which can result in spontaneous ignition. This investigation considers the self-heating process that occurs in a compost pile using a two-dimensional spatially-dependent model incorporating terms that account for self-

heating due to both biological and oxidative mechanisms. The variation of temperature distribution within different pile geometries is examined.

## Contents

<b>1</b>	<b>Introduction</b>	<b>C16</b>
<b>2</b>	<b>Mathematical formulation</b>	<b>C18</b>
<b>3</b>	<b>Results</b>	<b>C20</b>
<b>4</b>	<b>Conclusions</b>	<b>C23</b>
<b>5</b>	<b>Nomenclature</b>	<b>C23</b>

## 1 Introduction

As the result of growing environmental concerns, industrial composting has become one of the most essential techniques for dealing with the expanding volume of bio-waste. The oxidation of cellulosic materials and biological activity are often two drivers of heat generation in industrial compost piles, which contain enormous amounts of bulk organic materials [20]. The oxidation process represents chemical heat generation and may be modelled by a single Arrhenius reaction [1], whereas biological heat generation processes include the growth and respiration of microorganisms such as aerobic mould-fungi and bacteria. This biological heating, which takes place at lower temperatures than oxidation, can raise the temperature to a high enough level to ‘kick-start’ oxidation reactions. It is known to play a role in large-scale composting operations [20] and the storage of industrial waste fuels, such as municipal solid waste and landfill [6]. Self-heating due to biological activity is desirable in composting because it is the major mechanism that ‘decomposes’ organic materials within a pile into beneficial by-products [2]. Biological activity is known to work efficiently in the elevated temperature range of 50 to 90°C

which can be reached in compost materials within a few months or even a few days [5].

Sidhu, Nelson, and Chen [21] developed a spatial model that describes the temperature and oxygen concentrations in a compost pile. They investigated a two-dimensional rectangular compost pile and showed that the compost pile needs to be sufficiently large to be able to reach the elevated temperature range, which is the desirable condition for the biodegradation process (approximately 320–360 K) [20]. A larger pile increases the likelihood of reaching the typical cellulosic material ignition temperature point (423 K) [20]. Escudey et al. [3] and Moraga et al. [18] showed explicitly, based on experimental data from a sewage sludge pile, that this model provides reasonable predictions of temperature increases in a pile. Later Luangwilai et al. [13, 14, 15] extended the model of Sidhu, Nelson, and Chen [21] to investigate the effects of airflow over a wide range of speeds. They discovered that if the air speed is too high, heat loss dominates, requiring very large pile sizes to obtain the desirable temperature. In contrast, if the air speed is too low, the internal heat generated by the oxidation reaction stops once all oxygen has been used. Although for intermediate values of the air speed, elevated temperatures can be achieved by moderately sized compost piles, there is also the possibility of these piles spontaneously igniting. Luangwilai et al. [9, 12, 16] extended the model further to investigate the impact of moisture on the self-heating process in a compost pile when there is no airflow. Luangwilai, Sidhu, and Nelson [10, 11] and Luangwilai et al. [17] also investigated the model when both airflow and moisture are present. Moisture content is believed to be one of the most important aspects influencing the composting process because it is a necessary component for all microorganisms in a pile, without it the decomposition process slows down and becomes ineffective [4, 7, 20]. However, when there is too much moisture, the temperature of the compost remains low, which is not ideal for the biological reaction.

In this study, the mathematical model of Luangwilai et al. [17] is used to investigate the impact of compost pile geometry on the self-heating process. The overall goal of this study is to gain better knowledge of how a compost

pile self-heats.

## 2 Mathematical formulation

The critical effects of the boundaries and the actual geometry of the compost pile are not captured by the one-dimensional model. Therefore a two-dimensional model is used in this study for a better understanding of geometry and boundary effects. The compost pile is considered to be an infinitely long triangular, trapezoidal or rectangular slab (as can be seen in Figure 1) with thickness (width)  $L$ , and height  $H$ . The governing dimensional equations that describe the time-dependent temperature  $T$ , oxygen concentration  $O_2$ , vapour concentration  $V$ , and liquid water concentration  $W$  in the  $0 \leq x \leq L$  and  $0 \leq y \leq H$  domain are given below.

Governing equations:

$$\begin{aligned}
 (\rho C)_{\text{eff}} \frac{\partial T}{\partial t} &= k_{\text{eff}} \left( \frac{\partial^2 T}{\partial x^2} + \frac{\partial^2 T}{\partial y^2} \right) - \epsilon \rho_{\text{air}} C_{\text{air}} \left( u_x \frac{\partial T}{\partial x} + u_y \frac{\partial T}{\partial y} \right) \\
 &\quad + \mu_1(W) Q_c \rho_c A_3 O_2 M_{O_2} (1 - \epsilon) e^{-E_3/RT} \\
 &\quad + \mu_2(W) Q_b \rho_b (1 - \epsilon) \frac{A_1 e^{-E_1/RT}}{1 + A_2 e^{-E_2/RT}} \\
 &\quad + L_v [\epsilon Z_c V - (1 - \epsilon) Z_e W e^{-L_v/RT}], \tag{1}
 \end{aligned}$$

$$\begin{aligned}
 \epsilon \frac{\partial O_2}{\partial t} &= D_{O_2 \text{eff}} \left( \frac{\partial^2 O_2}{\partial x^2} + \frac{\partial^2 O_2}{\partial y^2} \right) - \epsilon \left( u_x \frac{\partial O_2}{\partial x} + u_y \frac{\partial O_2}{\partial y} \right) \\
 &\quad - \mu_1(W) \rho_c A_3 O_2 (1 - \epsilon) e^{-E_3/RT}, \tag{2}
 \end{aligned}$$

$$\begin{aligned}
 \epsilon \frac{\partial V}{\partial t} &= D_V \left( \frac{\partial^2 V}{\partial x^2} + \frac{\partial^2 V}{\partial y^2} \right) - \epsilon \left( u_x \frac{\partial V}{\partial x} + u_y \frac{\partial V}{\partial y} \right) - \epsilon Z_c V \\
 &\quad + (1 - \epsilon) Z_e W e^{-L_v/RT}, \tag{3}
 \end{aligned}$$

$$(1 - \epsilon) \frac{\partial W}{\partial t} = \epsilon Z_c V - (1 - \epsilon) Z_e W e^{-L_v/RT}. \tag{4}$$

Algebraic relationships:

$$k_{\text{eff}} = \epsilon k_{\text{air}} + (1 - \epsilon) [\sigma k_w + (1 - \sigma) k_c], \quad (5)$$

$$(\rho C)_{\text{eff}} = \epsilon \rho_{\text{air}} C_{\text{air}} + (1 - \epsilon) (W M_w C_w + \rho_{\text{compost}} C_c), \quad (6)$$

$$D_{O_2\text{eff}} = D_V = \epsilon D_{O_2\text{air}}, \quad (7)$$

$$\mu_1(W) = \begin{cases} 1 - (W/W_c)^b, & W < W_c, \\ 0, & W \geq W_c, \end{cases} \quad (8)$$

$$\mu_2(W) = \begin{cases} (\sigma - \sigma_a) / (\sigma_m - \sigma_a), & \sigma_a \leq \sigma \leq \sigma_m, \\ (\sigma_b - \sigma) / (\sigma_b - \sigma_m), & \sigma_m \leq \sigma \leq \sigma_b, \\ 0, & \text{otherwise.} \end{cases} \quad (9)$$

Laplace's equation for the stream function:

$$\frac{\partial^2 \Psi}{\partial x^2} + \frac{\partial^2 \Psi}{\partial y^2} = 0. \quad (10)$$

The terms in equations (1) to (10) are in defined the nomenclature in Section 5 and further details of each term are given by Luangwilai et al. [11, 17]. The heat generated by oxidation of the cellulosic materials is represented by the term containing the function  $\mu_1(W)$  on the right-hand sides of equations (1) and (2). The heat generated by biological activity is represented by the term containing the function  $\mu_2(W)$  on the right-hand side of equation (1).

Equations (3) and (4) represent the evaporation and condensation processes within the compost pile, respectively, with the energy change from these reactions represented by the term with coefficient  $L_v$  in equation (1). The  $\epsilon Z_c V$  terms on the right-hand sides of equations (3) and (4) represents the rate of condensation, and the  $(1 - \epsilon) Z_c W e^{-L_v/RT}$  terms relate to the rate of evaporation.

The diffusion and the effect of the airflow are defined by the first and the second terms on the right-hand sides of equations (1)–(3), respectively. The algebraic expressions (5) and (6) define the effective thermal conductivity and effective thermal capacity of the compost pile, respectively, in terms of the

corresponding properties of the air, compost materials, and moisture content. Equation (7) defines the effective diffusion coefficients for oxygen and vapour. The effects of moisture on the oxidation and biological reactions are defined in equations (8) and (9), respectively.

We assume simple boundary conditions for the system. The values of the temperature, oxygen and vapour are assumed to be ambient, that is,  $T = T_a$ ,  $O_2 = O_{2,a}$  and  $V = V_a$  at the left and right boundaries. The parameter values, which are based on those used by Sidhu, Nelson, and Chen [21] and Kuwahara et al. [7], are provided in the nomenclature in Section 5.

### 3 Results

This section presents the results from the numerical investigation of the governing equations (1) to (4), and their corresponding boundary conditions, using the software package FlexPDE<sup>TM</sup> [19]. FlexPDE<sup>TM</sup> is a commercial finite-element package for obtaining numerical solutions to partial differential equations. The numerical results from FlexPDE<sup>TM</sup> have been verified previously using finite differences and the method of lines [8, 21].

In this investigation, we set the airflow velocity  $\mathbf{U} = 1 \times 10^{-5} \text{ ms}^{-1}$ , which is between the two extreme flow rates,  $\mathbf{U} = 1 \times 10^{-6} \text{ ms}^{-1}$  and  $\mathbf{U} = 1 \times 10^{-2} \text{ ms}^{-1}$ , in the study of Luangwilai et al. [15]. The initial moisture content within the pile is set to 50% so the liquid water-to-compost weight ratio is  $\sigma(0) = 0.5$ , which is the intermediate value from Luangwilai et al. [9, 12, 16]. This  $\sigma$  value means that there is sufficient moisture for the biological reaction but at the same time there is not too much to cover the reaction site (compost material surface).

For each case the pile's base width is set to  $L = 20 \text{ m}$ , which is wide enough to ensure that the temperature can rise to the elevated temperature range of approximately 320–360 K (an observation based on our earlier studies). The angle at the base of the compost pile  $\theta$  is adjusted from  $60^\circ$  to  $90^\circ$  to study the effect of compost pile shape. The compost pile is considered

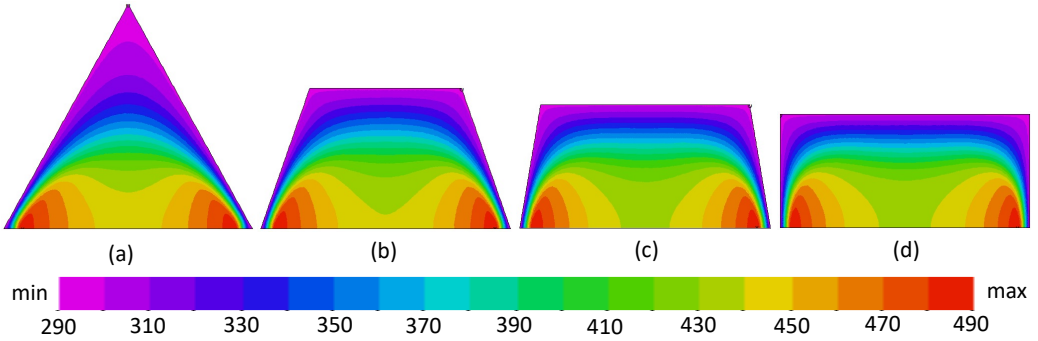


Figure 1: Two-dimensional steady-state temperature distributions within compost piles. The angles at the base of compost pile  $\theta$  are: (a)  $60^\circ$ ; (b)  $70^\circ$ ; (c)  $80^\circ$ ; and (d)  $90^\circ$ . The base width of compost piles are fixed at 20 m.

to be triangular when  $\theta = 60^\circ$ . The compost pile is considered to be a trapezoidal configuration when  $60^\circ < \theta < 90^\circ$ . Finally, a rectangular shape of the compost pile is assumed when  $\theta = 90^\circ$ . In this study, the volume of the compost pile is kept the same for all cases. As a result, the height of the compost pile  $H$  varies between  $5\sqrt{3}$  and  $10\sqrt{3}$  m.

The steady-state temperature distribution within a compost pile is shown in Figure 1 for base angles  $60^\circ$ ,  $70^\circ$ ,  $80^\circ$ , and  $90^\circ$ , with the respective pile heights 17.3205 m, 10.7719 m, 9.4471 m, and 8.6603 m. Despite the differences in geometry, the steady-state temperature distributions for all cases are similar, with the same minimum and maximum temperature ranges. There are two hot spots in these temperature distributions, both around the compost pile's lower corners. This is because the oxidation reaction has consumed all of the oxygen in the centre of the compost pile, but the supply of air from the left and right borders maintains oxidation and keeps the lower corners warm. This type of behaviour is seen for all cases.

At the steady-state temperature the oxygen within the compost pile has been consumed by the oxidation reaction. The minimum oxygen concentration

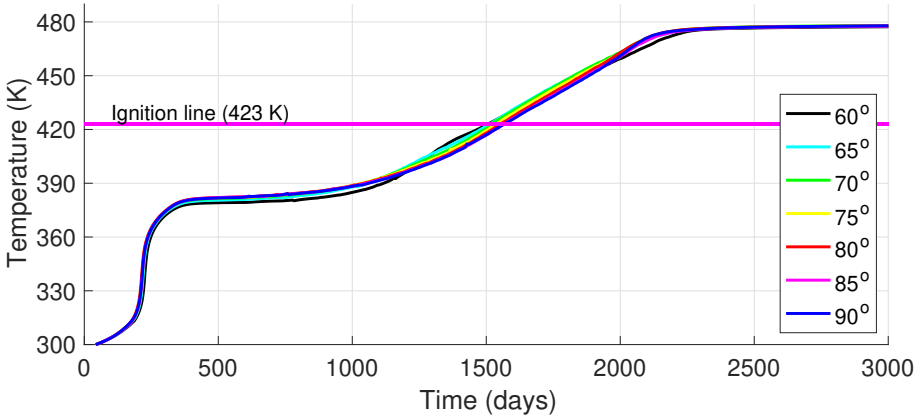


Figure 2: Time profiles of maximum temperature when the angle  $\theta$  at the bases of the composts are  $60^\circ$ ,  $65^\circ$ ,  $70^\circ$ ,  $75^\circ$ ,  $80^\circ$ ,  $85^\circ$ , and  $90^\circ$ .

point is located in the center of the pile. We observed that the water inside the compost pile has evaporated and the steady-state distributions are similar to the oxygen concentration.

The temperature profiles for different geometries are now compared. The maximum temperature profiles for compost piles with base angles  $\theta = 60^\circ$ ,  $65^\circ$ ,  $70^\circ$ ,  $75^\circ$ ,  $80^\circ$ ,  $85^\circ$ , and  $90^\circ$  are displayed versus time in Figure 2. The profiles of these cases are found to be nearly identical.

In Figure 2, the temperature profiles of all compost configurations reach the desirable temperature range (approximately 320–360 K) within 190 days. The temperature profiles remain at 380–390 K for approximately 500 days. The maximum temperature profile then continues to rise until it reaches the ignition temperature value at around 1400 days.

Overall when the volume and base width of the compost pile are fixed, variations in the geometry of the compost pile have little effect on the compost pile's behaviour and temperature profile. Unlike the study from Sidhu, Nelson, and Chen [21], as the size of the compost pile (adding more volume) is raised,

the temperature profile approaches the desirable temperature range faster and the risk of reaching the common ignition temperature range increases.

## 4 Conclusions

In this article, we investigated the self-heating of compost piles with various compost pile geometries using a two-dimensional spatially dependent model. Self-heating due to biological and oxidation reactions, the presence of moisture in both liquid and vapour forms, and airflow speeds were all included in the model. The angle at the base  $\theta$  was adjusted from  $60^\circ$  to  $90^\circ$  to investigate the effect of compost pile geometries on the self-heating process and compost pile behaviour. The geometries considered are triangle ( $\theta = 60^\circ$ ), trapezoid ( $60^\circ < \theta < 90^\circ$ ) and rectangle ( $\theta = 90^\circ$ ). The volume and compost base width  $L$  are kept constant in each case. As a result, the compost pile's height  $H$  varies.

The geometry has little effect on the compost pile behaviour. Every case has a similar temperature distribution. Furthermore, the maximum temperature profiles are remarkably similar. By combining the results of previous studies and this investigation, it is clear that the volume of the compost material plays a significant role rather than the geometry of the compost pile in terms of heat generation (the greater the volume, the faster the heat generation process). The current study will be expanded to incorporate new three-dimensional formulations of self-heating processes in compost piles.

## 5 Nomenclature

Table 1: Definitions and values of parameters in equations (1) to (10).

$A_1$	Pre-exponential factor for oxidation of biomass growth ( $2.0 \times 10^8 \text{ s}^{-1}$ )
-------	---

$A_2$	Pre-exponential factor for inhibition of biomass growth ( $6.86 \times 10^{30}$ )
$A_3$	Pre-exponential factor for oxidation of cellulosic material ( $1 \times 10^7 \text{ m}^3 \text{ kg}^{-1} \text{ s}^{-1}$ )
$b$	Constant for moisture covering effects (1.5)
$C_{\text{air}}$	Heat capacity of air ( $1005 \text{ J kg}^{-1} \text{ K}^{-1}$ )
$C_c$	Heat capacity of cellulosic material ( $3320 \text{ J kg}^{-1} \text{ K}^{-1}$ )
$C_w$	Heat capacity of water ( $4190 \text{ J kg}^{-1} \text{ K}^{-1}$ )
$D_{O_{2\text{air}}}$	Diffusion coefficient for oxygen ( $2.5 \times 10^{-5} \text{ m}^2 \text{ s}^{-1}$ )
$D_{O_{2\text{eff}}}$	Effective diffusion coefficient for oxygen ( $7.5 \times 10^{-6} \text{ m}^2 \text{ s}^{-1}$ )
$E_1$	Activation energy for biomass growth ( $100 \times 10^3 \text{ J mol biomass}^{-1}$ )
$E_2$	Activation energy for inhibition of biomass growth ( $200.0 \times 10^3 \text{ J mol biomass}^{-1}$ )
$E_3$	Activation energy for oxidation of cellulosic material ( $110 \times 10^3 \text{ J, mol}^{-1}$ )
$O_2$	Oxygen concentration within pile ( $\text{mol m}^{-3}$ )
$O_{2a}$	Ambient oxygen concentration ( $8.5675 \text{ mol m}^{-3}$ )
$Q_b$	Exothermicity for oxidation of biomass ( $6.66 \times 10^6 \text{ J kg}^{-1}$ )
$Q_c$	Exothermicity for oxidation of cellulosic material ( $1.7 \times 10^7 \text{ J kg}^{-1}$ )
$R$	Ideal gas constant ( $8.31441 \text{ J K}^{-1} \text{ mol}^{-1}$ )
$RH$	Relative humidity percentage (50%)
$T_a$	Ambient temperature (298 K)
$U$	Air velocity ( $\text{ms}^{-1}$ )
$k_{\text{air}}$	Effective thermal conductivity of air ( $0.026 \text{ W m}^{-1} \text{ K}^{-1}$ )
$k_c$	Effective thermal conductivity of cellulose ( $0.3 \text{ W m}^{-1} \text{ K}^{-1}$ )

$k_w$	Effective thermal conductivity of water (0.58 Wm <sup>-1</sup> K <sup>-1</sup> )
$k_{\text{eff}}$	Effective thermal conductivity of bed (Wm <sup>-1</sup> K <sup>-1</sup> )
$M_w$	Mass of water (0.018 kg mol <sup>-1</sup> )
$M_{O_2}$	Mass of oxygen (0.032 kg mol <sup>-1</sup> )
$V_a$	Ambient water vapour concentration (1.74 × RH mol m <sup>-3</sup> )
$W_c$	Critical liquid water effectively covering all site (300/0.018 mol m <sup>-3</sup> )
$Z_c$	Pre-exponential factor for condensation (4.7 s <sup>-1</sup> )
$Z_e$	Pre-exponential factor for evaporation (3.41 × 10 <sup>4</sup> s <sup>-1</sup> )
$L_v$	Latent heat of vapourisation (42 × 10 <sup>3</sup> J mol <sup>-1</sup> )
$\epsilon$	Void fraction (0.3)
$(\rho C)_{\text{eff}}$	Effective thermal capacity per unit volume of bed (J m <sup>-3</sup> K <sup>-1</sup> )
$\rho_{\text{air}}$	Density of air (1.17 kg m <sup>-3</sup> )
$\rho_b$	Density of bulk biomass within compost pile (120 kg m <sup>-3</sup> )
$\rho_c$	Density of pure cellulosic material (120 kg m <sup>-3</sup> )
$\rho_{\text{compost}}$	Density of bulk biomass within compost pile (120 kg m <sup>-3</sup> )
$\rho_w$	Density of water (1000 kg m <sup>-3</sup> )
$\sigma$	Liquid water-to-compost weight ratio $WM_w/[WM_w + (1 - \epsilon)\rho_{\text{compost}}]$
$\sigma_a$	Activation limit of liquid water-to-compost weight ratio (0.15)
$\sigma_m$	Optimum limit of liquid water-to-compost weight ratio (0.6)
$\sigma_b$	Deactivation limit of liquid water-to-compost weight ratio (0.8)

## References

- [1] P. C. Bowes. *Self heating: evaluating and controlling the hazard*. Amsterdam: Elsevier Press, 1984 (cit. on p. [C16](#)).
- [2] W. F. Brinton, Jr. E. Evans, M. L. Droffner, and R. B. Brinton. “Standardized test for evaluation of compost self-heating”. In: *BioCycle* 36 (1995), pp. 60–65 (cit. on p. [C16](#)).
- [3] M. Escudey, A. Arias, J. Forster, N. Moraga, C. Zambra, and A. C. Chang. “Sewage sludge self-heating and spontaneous combustion. Field, laboratory and numerical studies”. In: *High Temp. Mater. Proc.* 27.5 (2008), pp. 337–346. DOI: [10.1515/HTMP.2008.27.5.337](#) (cit. on p. [C17](#)).
- [4] R. T. Haug. *The Practical Handbook of Compost Engineering*. USA: Lewis Publishers, 1993. DOI: [10.1201/9780203736234](#) (cit. on p. [C17](#)).
- [5] W. Hogland, T. Bramryd, and I. Persson. “Physical, biological and chemical effects of unsorted fractions of industrial solid waste in waste fuel storage”. In: *Waste Manage. Res.* 14.2 (1996), pp. 197–210. DOI: [10.1006/wmre.1996.0019](#) (cit. on p. [C17](#)).
- [6] P. F. Hudak. “Spontaneous combustion of shale spoils at sanitary landfill”. In: *Waste Manage. Res.* 22.6 (2002), pp. 687–688. DOI: [10.1016/s0956-053x\(01\)00077-0](#) (cit. on p. [C16](#)).
- [7] F. Kuwahara, Y. Sano, A. Nakayama, K. Nakasaki, and T. Fukazawa. “Numerical modelling of a composting process with aeration”. In: *J. Porous Media* 12.10 (2009), pp. 927–938. DOI: [10.1615/JPorMedia.v12.i10.10](#) (cit. on pp. [C17](#), [C20](#)).
- [8] T. Luangwilai and H. S. Sidhu. “Determining critical conditions for two dimensional compost piles with air flow via numerical simulations”. In: *Proceedings of the 15th Biennial Computational Techniques and Applications Conference, CTAC-2010*. Ed. by W. McLean and A. J. Roberts. Vol. 52. ANZIAM J. 2011, pp. C463–C481. DOI: [10.21914/anziamj.v52i0.3753](#) (cit. on p. [C20](#)).

- [9] T. Luangwilai, H. S. Sidhu, and M. I. Nelson. “A two dimensional, reaction-diffusion model of compost piles”. In: *Proceedings of the 10th Biennial Engineering Mathematics and Applications Conference, EMAC-2011*. Ed. by M. Nelson, M. Coupland, H. Sidhu, T. Hamilton, and A. J. Roberts. Vol. 53. ANZIAM J. 2012, pp. C34–C52. DOI: [10.21914/anziamj.v53i0.5083](https://doi.org/10.21914/anziamj.v53i0.5083) (cit. on pp. C17, C20).
- [10] T. Luangwilai, H. S. Sidhu, and M. I. Nelson. “One-dimensional spatial model for self-heating in compost piles: Investigating effects of moisture and air flow”. In: *Food Bioprod. Process.* 108 (2018), pp. 18–26. DOI: [10.1016/j.fbp.2017.12.001](https://doi.org/10.1016/j.fbp.2017.12.001) (cit. on p. C17).
- [11] T. Luangwilai, H. S. Sidhu, and M. I. Nelson. “Understanding effects of ambient humidity on self-heating of compost piles”. In: *CHEMECA 2018*. Institution of Chemical Engineers. 2018, p. 68. URL: <https://search.informit.org/doi/10.3316/informit.049196748938234> (cit. on pp. C17, C19).
- [12] T. Luangwilai, H. S. Sidhu, and M. I. Nelson. “Understanding the role of moisture in the self-heating process of compost piles”. In: *CHEMECA 2012*. Engineers Australia. 2012, pp. 1834–1846. URL: <https://search.informit.org/doi/10.3316/INFORMIT.867764346204981> (cit. on pp. C17, C20).
- [13] T. Luangwilai, H. S. Sidhu, M. I. Nelson, and X. D. Chen. “Biological self-heating of compost piles with airflow”. In: *CHEMECA 2009*. Engineers Australia. 2009, pp. 2683–2692. URL: <https://search.informit.org/doi/10.3316/informit.799299549211365> (cit. on p. C17).
- [14] T. Luangwilai, H. S. Sidhu, M. I. Nelson, and X. D. Chen. “Modelling air flow and ambient temperature effects on the biological self-heating of compost piles”. In: *Asia-Pacific J. Chem. Eng.* 5.4 (2010), pp. 609–618. DOI: [10.1002/apj.438](https://doi.org/10.1002/apj.438) (cit. on p. C17).

- [15] T. Luangwilai, H. S. Sidhu, M. I. Nelson, and X. D. Chen. “Modelling the effects of air flow, ambient temperature and radiative boundary conditions in compost piles”. In: *CHEMECA 2010*. Engineers Australia. 2010, pp. 3585–3596. URL: <https://search.informit.org/doi/10.3316/informit.484992904303574> (cit. on pp. C17, C20).
- [16] T. Luangwilai, H. S. Sidhu, M. I. Nelson, and X. D. Chen. “Modelling the effects of moisture content in compost piles”. In: *CHEMECA 2011*. Engineers Australia. 2011, pp. 1473–1484. URL: <https://search.informit.org/doi/10.3316/informit.174710980721893> (cit. on pp. C17, C20).
- [17] T. Luangwilai, S. D. Watt, S. Fu, H. S. Sidhu, and M. I. Nelson. “Modelling the effects of ambient temperature variation on self-heating process of compost piles”. In: Engineers Australia (2019), pp. 84–96. URL: <https://search.informit.org/doi/10.3316/informit.689351109484953> (cit. on pp. C17, C19).
- [18] N. O. Moraga, F. Corvalan, M. Escudey, A. Arias, and C. E. Zambra. “Unsteady 2D coupled heat and mass transfer in porous media with biological and chemical heat generations”. In: *Int. J. Heat Mass Trans.* 52 (2009), pp. 5841–5848. DOI: [10.1016/j.ijheatmasstransfer.2009.07.027](https://doi.org/10.1016/j.ijheatmasstransfer.2009.07.027) (cit. on p. C17).
- [19] PDE Solutions Inc. *FlexPDE v 6.05*. PDE Solutions Inc. Cambridge MA, 2009. URL: <http://www.pdesolutions.com> (cit. on p. C20).
- [20] R. Rynk. “Fires at composting facilities: causes and conditions Part I”. In: *BioCycle* 41.1 (2000), pp. 54–58 (cit. on pp. C16, C17).
- [21] H. S. Sidhu, M. I. Nelson, and X. D. Chen. “A simple spatial model for self-heating compost piles”. In: *Proceedings of the 13th Biennial Computational Techniques and Applications Conference, CTAC-2006*. Ed. by W. Read and A. J. Roberts. Vol. 48. ANZIAM J. 2007,

pp. C135–C150. DOI: [10.21914/anziamj.v48i0.86](https://doi.org/10.21914/anziamj.v48i0.86) (cit. on pp. C17, C20, C22).

## Author addresses

1. **T. Luangwilai**, Mathematics and Computer Science Division, Navaminda Kasatriyadhiraj Royal Thai Air Force Academy, Bangkok, 10220, THAILAND.  
<mailto:thiansiri.l@gmail.com>
2. **H. S. Sidhu**, Applied and Industrial Mathematics Research Group (AIM), School of Science, University of New South Wales at the Australian Defence Force Academy Canberra, ACT, 2600 AUSTRALIA.
3. **M. I. Nelson**, School of Mathematics and Applied Statistics, University of Wollongong, Wollongong, NSW, 2522 AUSTRALIA.